ACS chemical biology

pubs.acs.org/acschemicalbiology

Article

Biochemical Characterization of Disease-Associated Variants of Human Ornithine Transcarbamylase

Emily Micheloni, Samantha S. Watson, Penny J. Beuning,* and Mary Jo Ondrechen*

Cite This: *ACS Chem. Biol.* 2025, 20, 1059−1067

Read Online

ACCESS | Metrics & More | Article Recommendations | Supporting Information

ABSTRACT: Human ornithine transcarbamylase deficiency (OTCD) is the most common ureagenesis disorder in the world. OTCD is an X-linked genetic deficiency in which patients experience hyperammonemia to varying degrees depending on the severity of the genetic mutation. More than two-thirds of the known mutations are caused by single nucleotide substitutions. In this paper, partial order optimum likelihood (POOL), a machine learning method, is used to analyze single nucleotide substitutions in OTC with varying disease phenotypes and predicted catalytic efficiencies. Specifically, we used a computed metric, μ_4, a measure of the degree of coupling between an ionizable residue and its neighbors, calculated for the catalytic residues, to identify which protein variants were most likely to have impacted catalytic activities. From this analysis, 17 disease-associated variants were selected plus one additional variant, representing a range of μ_4 values and POOL ranks. Then μ_4 predictions were compared with established bioinformatics tools, SIFT, PolyPhen-2, Provean, FATHMM, MutPred2, and MutationTaster2. The bioinformatics tools predicted that most of these mutations are deleterious. The variants were biochemically characterized using kinetics assays, size exclusion chromatography, and differential scanning fluorimetry. POOL combined with μ_4 analysis was able to predict correctly which variants were catalytically hindered in vitro for 17 out of 18 variants. Then by expressing a subset of these proteins in cell culture, mechanisms for disease were proposed. Analysis using μ_4 is a complementary method to the sequence-based bioinformatics tools for predicting the effects of mutation on catalytic function.

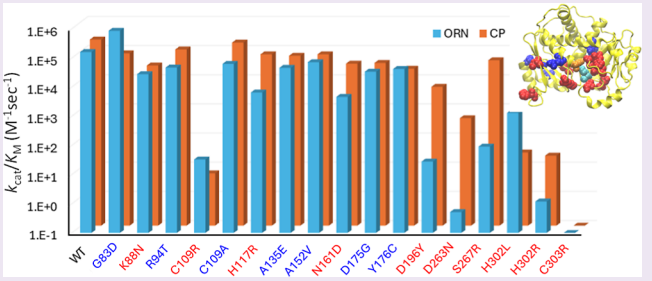

Every year, 14,000−77,000 individuals are diagnosed with ornithine transcarbamylase deficiency, OTCD, making it the most common ureagenesis disorder.[1] OTCD is an X-linked genetic disorder that usually results in the inability to metabolize excess ammonia. OTC catalyzes the formation of citrulline from ornithine and carbamoyl phosphate, in a key step in the urea cycle; the formation of citrulline is also an important step in the biosynthesis of arginine. Disease carriers accumulate nitrogenous waste in their bloodstream resulting in symptoms such as vomiting, lethargy, coma, cerebral edema and, if left untreated, death.[2] The severity of the symptoms depends on the mutation and the deficiency of the enzyme.[3]

Generally, OTCD can be classified by disease onset, as (1) neonatal (2) late (3) female. The most severe form of the disease is neonatal onset in which newborns experience symptoms during the first week of life. These patients often have very poor outcomes, including neurological damage.[4] However, males with late onset can exhibit a milder phenotype which presents months or years after birth.[5] The widest range of phenotypic variability occurs with female onset due to random X chromosome inactivation. Therefore, the specific mutation present can play a large role in the clinical manifestation, which ranges from apparent normality to severe neurological impairments.[4,6,7]

Currently, the Human Gene Mutation Database reports 486 mutations in the human OTC gene.[8] Single nucleotide base pair substitutions make up the 332 missense and nonsense mutations.[9−11] Despite the available genetic information, little biochemical characterization of these disease associated proteins has been reported. Using the computational tool developed by us, partial order optimum likelihood, POOL,[12] we analyzed the known disease-associated variants resulting from these point mutations.

POOL is a machine learning method that rank-orders a protein's amino acids by the probability of functional importance, for example, ligand binding or catalytic activity.[12] POOL uses THEoretical Microscopic Anomalous TItration Curve Shapes, THEMATICS, as input features to identify these important residues.[13] Briefly, THEMATICS computes theoretical titration curves for the ionizable residues in the structure and identifies residues with anomalous curves that are

Received: January 14, 2025
Revised: February 24, 2025
Accepted: March 3, 2025
Published: March 10, 2025

https://doi.org/10.1021/acschembio.5c00043
ACS Chem. Biol. 2025, 20, 1059−1067

Table 1. Summary of Predictions for hOTC Disease Associated Variants

Disease Onset	Mutation[a]	POOL rank	μ4[b]	SIFT[c]	PolyPhen-2[c]	Provean[c]	ΔΔG[d]
--	WT	--	--	---	---	---	---
Neonatal	G83D	119	Unaffected	Deleterious	Possibly Damaging	Deleterious	152
Late	K88N	14	Hindered	Deleterious	Damaging	Deleterious	50
Late	R94T	93	Unaffected	Deleterious	Damaging	Deleterious	62
Female	C109R	223	Hindered	Deleterious	Benign	Deleterious	227
N/A	C109A	223	Hindered	Tolerated	Benign	Neutral	17
Late	H117R	117	Hindered	Tolerated	Damaging	Neutral	-1
Late	A135E	299	Unaffected	Deleterious	Benign	Neutral	46
Late	A152V	294	Unaffected	Tolerated	Benign	Deleterious	57
Neonatal	N161D	116	Hindered	Deleterious	Damaging	Deleterious	79
Late	D175G	5	Unaffected	Deleterious	Damaging	Deleterious	-33
Late	Y176C	8	Unaffected	Deleterious	Damaging	Deleterious	72
Female	W193R**	42	Hindered	Deleterious	Damaging	Deleterious	-5
Neonatal	D196Y	23	Hindered	Deleterious	Damaging	Deleterious	-32
Female	D263N	2	Hindered	Deleterious	Damaging	Deleterious	-37
Female	S267R	28	Hindered	Deleterious	Damaging	Deleterious	-68
Late	H302L	3	Hindered	Deleterious	Damaging	Deleterious	-10
Neonatal	H302R	3	Hindered	Deleterious	Damaging	Deleterious	-5
Neonatal	C303R	1	Hindered	Deleterious	Damaging	Deleterious	-34

[a]The mutation is colored red if the fold decrease in activity is ≥10-fold with respect to either CP or ORN (Tables 2 and 3). The C109A mutation is not reported to be disease-associated and is included here due to subsequent analysis. [b]A summary of the μ_4 data based on our established cutoff. A mutation is considered hindered (green) if it has three or more catalytic residues with a change in μ_4 greater than 20%, or one catalytic residue with a change in μ_4 > 40% (details in Table S1). [c]Predictions from SIFT, PolyPhen-2, and Provean are shown (deleterious mutations are colored). Scoring details are in Table S2. [d]$\Delta\Delta G$ values were obtained from Desmond within Schrödinger. Pink highlights the variants with decreased stability with respect to WT OTC. [e]MutPred2 and FATHMM predicted all mutations to be deleterious (Tables S2 and S3). [f]Could not be purified in sufficient quantities for in vitro characterization.

characteristic of biochemically active residues. POOL utilizes binding pocket information from ConCavity[14] with THEMATICS metrics to generate its rank-ordered list. We have shown POOL to be a highly successful tool in identifying catalytically active residues, including distal residues.[15,16]

We focus here on a new method that investigates changes in the fourth central moment (μ_4) of the computed proton occupation curves of the known ionizable active site residues in the disease-associated variants of OTC, compared to WT. The value μ_4 is a THEMATICS metric and represents the "tailness" or kurtosis of the first derivative of the theoretical titration curve and is a measure of the degree of coupling of the protonation equilibrium with those of other ionizable amino acids. We have shown previously that μ_4 is the best predictor of the residues that are biochemically active[17] and have argued that, in a highly evolved enzyme, the μ_4 values of the catalytic amino acids are optimized.[18] We hypothesized that by comparing the changes in μ_4 between WT OTC and the disease-associated variants, we could predict which variants are catalytically hindered, if the catalytic residues show substantial changes in their μ_4 values. However, if the changes in μ_4 are small then the variant is not predicted to be catalytically hindered even if it is disease associated.

A recent report on 17 cancer-associated variants of human DNA polymerase kappa (pol κ) showed that eight of these variants had at least one of three catalytic residues (D107, D198, and E199) with a μ_4 value change of at least 50% relative to WT pol κ; these eight variants were observed to be catalytically hindered, whereas the other nine variants with smaller differences in μ_4 were kinetically similar to WT pol κ.[19] Here, we determined μ_4 values for the active site residues in WT OTC and variants and then compared the μ_4 analysis with predictions from informatics-based programs: SIFT, Polyphen-2, Provean, FATHMM, MutPred2, and MutationTaster2.[20−24,29] Our μ_4 analysis accurately predicted which of these variants are catalytically hindered in vitro. In addition, we determined the stability of these enzymes to hypothesize why some variants are disease associated even though they are catalytically similar to WT OTC in vitro. We also determined activity of these variants in human cell culture and found that the bioinformatics programs are better at predicting their phenotypes as expressed in mammalian cells.

RESULTS AND DISCUSSION

Analysis of μ_4 of Active Site Residues of OTC Disease Associated Variants. Our μ_4 analysis focused on the ionizable residues in the active site of hOTC. The CP binding domain was defined to include R92, R141, and H168. The phosphate binding motif is ^{90}SxRT; ^{168}HPxQ binds the carbamoyl moiety.[9,26] We define the ornithine binding domain as D263, H302, and C303 based on the conserved sequence of ^{301}LHCLP and known ornithine binding domain ^{263}DxxxSMG.[25,27,28] Even though these distinctions were made, some residues such as C303 can be involved in binding both ORN and CP.

All the studied variants except C109A had documented disease associated phenotypes.[1,11] Eight of these variants had changes in the μ_4 value of at least three active site residues (Table S1). Some of these residues were highly POOL ranked, for example C303, D263, and H302 were ranked first, second and third, respectively. While one would expect that mutation of one of the highest POOL-ranked residues such as C303, D263 and H302 would result in reduced activity, we hypothesized that alterations in the μ_4 values of the active

https://doi.org/10.1021/acschembio.5c00043
ACS Chem. Biol. 2025, 20, 1059−1067

Table 2. Steady-State Kinetics Assay Results for hOTC WT and Variants with Respect to ORN

POOL rank	variant	onset	K_m (mM)	V_{max} (mM/min)	k_{cat} (s^{-1})	k_{cat}/K_m (M^{-1} s^{-1})	fold decrease hOTC
	WT		0.37 ± 0.14	0.035 ± 0.0037	59 ± 12	$1.6 \times 10^5 \pm 2.4 \times 10^4$	
119	G83D	neonatal	0.82 ± 0.12	0.041 ± 0.0013	68 ± 0.50	$8.6 \times 10^4 \pm 1.8 \times 10^4$	1.9
14	K88N	late	2.8 ± 0.41	0.0090 ± 0.0021	7.5 ± 1.8	$2.8 \times 10^4 \pm 7.8 \times 10^4$	57
93	R94T	late	0.34 ± 0.057	0.0047 ± 0.0022	16 ± 2.2	$4.7 \times 10^4 \pm 6.5 \times 10^3$	3.4
223	C109R	female	0.56 ± 0.095	0.00032 ± 0.0000037	0.018 ± 0.0020	$3.3 \times 10^1 \pm 5.9$	4.9×10^3
223	C109A	N/A	0.75 ± 0.010	0.028 ± 0.0028	47 ± 4.7	$6.3 \times 10^4 \pm 1.1 \times 10^4$	2.5
117	H117R	late	0.57 ± 0.13	0.0045 ± 0.00025	3.7 ± 0.60	$6.5 \times 10^3 \pm 9.4 \times 10^2$	25
299	A135E	late	0.70 ± 0.054	0.038 ± 0.0098	32 ± 8.2	$4.6 \times 10^4 \pm 1.0 \times 10^4$	3.5
294	A152V	late	0.33 ± 0.055	0.027 ± 0.0016	23 ± 1.3	$7.2 \times 10^4 \pm 1.8 \times 10^4$	2.2
116	N161D	neonatal	3.4 ± 0.91	0.0046 ± 0.0010	15 ± 3.5	$4.6 \times 10^3 \pm 1.2 \times 10^3$	35
5	D175G	late	0.64 ± 0.060	0.026 ± 0.0033	22 ± 2.7	$3.4 \times 10^4 \pm 4.6 \times 10^3$	4.7
8	Y176C	late	0.40 ± 0.070	0.020 ± 0.00070	16 ± 0.59	$4.2 \times 10^4 \pm 9.2 \times 10^3$	3.8
23	D196Y	neonatal	55 ± 1.6	0.014 ± 0.00058	1.5 ± 0.065	$2.8 \times 10^1 \pm 1.1 + 01$	5.7×10^3
2	D263N	female	172 ± 29	0.0042 ± 0.00055	0.088 ± 0.011	$0.52 \pm 9.5 \times 10^{-2}$	3.1×10^5
28	S267R	female	42.7 ± 12	0.0093 ± 0.0010	3.9 ± 0.73	$9.1 \times 10^1 \pm 1.4 \times 10^1$	1.8×10^3
3	H302L	late	8.0 ± 1.9	0.024 ± 0.0018	10 ± 1.8	$1.3 \times 10^3 \pm 1.4 \times 10^2$	1.2×10^3
3	H302R	neonatal	96 ± 10	0.0020 ± 0.00032	0.12 ± 0.017	1.2 ± 0.051	1.3×10^5
1	C303R[a]	neonatal					

[a]OTC C303R had activity below the limit of detection for the assay which was calculated to be 0.3 μM citrulline formation.

Table 3. Steady-State Kinetics Assay Results for hOTC WT and Variants with Respect to CP

POOL rank	variant	onset	K_m (mM)	V_{max} (mM/min)	k_{cat} (s^{-1})	k_{cat}/K_m (M^{-1} s^{-1})	fold decrease hOTC
	WT		0.24 ± 0.07	0.034 ± 0.0022	56 ± 9.8	$2.4 \times 10^5 \pm 2.9 \times 10^4$	
119	G83D	neonatal	0.73 ± 0.069	0.035 ± 0.0064	58 ± 11	$8.1 \times 10^4 \pm 2.0 \times 10^4$	3.0
14	K88N	late	0.20 ± 0.024	0.0069 ± 0.0017	5.8 ± 1.4	$3.1 \times 10^4 \pm 1.2 \times 10^4$	5.2
93	R94T	late	0.15 ± 0.028	0.0047 ± 0.00023	16 ± 2.1	$1.1 \times 10^5 \pm 1.8 \times 10^4$	1.5
223	C109R	female	3.4 ± 0.31	0.00038 ± 0.0000057	0.021 ± 0.0031	6.2 ± 0.76	2.6×10^4
223	C109A	N/A	0.21 ± 0.036	0.023 ± 0.0020	39 ± 3.5	$1.9 \times 10^5 \pm 1.7 \times 10^4$	0.84
117	H117R	late	0.052 ± 0.0074	0.0047 ± 0.00078	3.9 ± 0.65	$7.5 \times 10^4 \pm 1.1 \times 10^3$	2.1
299	A135E	late	0.42 ± 0.028	0.034 ± 0.0086	28 ± 7.2	$6.7 \times 10^4 \pm 1.8 \times 10^4$	2.4
294	A152V	late	0.29 ± 0.023	0.026 ± 0.0019	22 ± 1.5	$7.5 \times 10^4 \pm 5.0 \times 10^3$	2.2
116	N161D	neonatal	0.37 ± 0.04	0.0040 ± 0.00068	13 ± 2.3	$3.6 \times 10^4 \pm 3.2 \times 10^3$	4.4
5	D175G	late	0.54 ± 0.063	0.025 ± 0.0028	21 ± 2.4	$3.8 \times 10^4 \pm 2.8 \times 10^3$	4.2
8	Y176C	late	0.53 ± 0.078	0.056 ± 0.0012	12 ± 0.98	$2.4 \times 10^4 \pm 2.6 \times 10^3$	6.7
23	D196Y	neonatal	0.21 ± 0.017	0.011 ± 0.00054	1.2 ± 0.060	$5.7 \times 10^3 \pm 3.2 \times 10^2$	28
2	D263N	female	0.54 ± 0.18	0.012 ± 0.0020	0.25 ± 0.038	$4.8 \times 10^2 \pm 8.5 \times 10^1$	3.3×10^2
28	S267R	female	0.061 ± 0.013	0.0067 ± 0.00025	2.8 ± 0.10	$4.7 \times 10^4 \pm 1.8 \times 10^3$	3.4
3	H302L	late	5.5 ± 1.2	0.023 ± 0.0028	9.5 ± 1.2	$1.8 \times 10^3 \pm 2.4 \times 10^2$	89
3	H302R	neonatal	3.8 ± 0.91	0.0015 ± 0.00024	0.116 ± 0.013	$3.2 \times 10^1 \pm 6.9$	5.0×10^3
1	C303R[a]	neonatal					

[a]OTC C303R had activity below the limit of detection for the assay which was calculated to be 0.3 μM citrulline formation.

site residues are better predictors of loss of activity. A residue with a low POOL ranking, such as C109 (rank 223) and N161 (rank 116), when mutated to an amino acid with very different electrostatic properties, for instance in the variants C109R and N161D, could alter the electrical potential at one or more of the active site residues and thus affect activity. Furthermore, while a loss of stability that is large enough to cause unfolding would be detrimental to activity, we do not expect smaller changes in stability to be strongly correlated with activity because active sites are local regions of higher energy that enable catalysis. Therefore, we expected that the best predictor of loss of activity is many changes or larger changes in the μ_4 of the active site residues. To test this hypothesis, residues that had small changes in μ_4 and different disease phenotypes were also chosen: G83D, R94T, A135E, A152V, D175G, and Y176C. We predicted that these variants would not be catalytically hindered even though residues D175 and Y176 were highly POOL ranked, fifth and eighth, respectively. Other variants such as D196Y and H302L were chosen to determine if a cutoff in μ_4 could be identified, since these variants only had one residue with a μ_4 change greater than 40%. N161D was analyzed because it had the greatest change in a single μ_4 value of all the variants.

These 18 variants were also analyzed with other methods that are bioinformatics based, SIFT, PolyPhen-2, Provean, FATHMM, MutPred2, and MutationTaster2. SIFT uses multiple sequence alignments to predict tolerated and deleterious substitutions for every amino acid in the sequence, then calculates the normalized probabilities for all possible substitutions.[20] PolyPhen-2 is a prediction tool that uses sequence-based features combined with structural features to predict whether the amino acid substitution is damaging.[21] Similarly, Provean is also based on multiple sequence alignments and conservation scores to determine if protein

https://doi.org/10.1021/acschembio.5c00043
ACS Chem. Biol. 2025, 20, 1059−1067

sequence variation affects protein function.[23] FATHMM, Functional Analysis through Hidden Markov Models, is based on amino acid sequence and conserved amino acids.[22] MutPred2 is a sequence-based model that uses machine learning to provide probable reasons for the pathogenicity of amino acid substitutions.[24] Finally, MutationTaster2[29] incorporates evolutionary conservation, splice-site changes and effects on protein features and mRNA.[30] Detailed results from the bioinformatics servers are in Supporting Information (Tables S2 and S3).

Table 1 summarizes the POOL analysis and bioinformatics results of hOTC variants. SIFT predicted that of the variants analyzed, only C109A, H117R, and A152V would be tolerated. PolyPhen-2 predicted only C109R, C109A, A135E, and A152V as benign mutations. Provean predicted all mutations to be deleterious except C109A, H117R, and A135E would be neutral. C109A, which is not a disease associated mutation, was predicted to be tolerated by all the servers except FATHMM.

A significant decrease in catalytic activity is observed for mutations that cause changes in μ_4 of at least 40% in one active residue or with three or more active residues with μ_4 change greater than 20% compared to WT OTC (Tables 2 and 3, Table S1). Using these μ_4 parameters allowed correct prediction of most variants that were catalytically hindered in vitro except for W193R and C109A. OTC W193R was predicted to be catalytically deficient but it could not be produced in sufficient quantities for assays. OTC C109A was predicted to be catalytically deficient with a 78% change in μ_4 of R92 (Table S1) but was catalytically similar to WT OTC (Tables 2 and 3), the only incorrect prediction by the μ_4 metric. It is possible that a change in μ_4 might be better tolerated in some active site residues than others. For example, the change in μ_4 of D263, which is ranked second using POOL, might be less tolerated than a change in μ_4 of R92, which is ranked 11th. Thus, this prediction method may benefit from the POOL rank and change in μ_4 of these residues (Table 1).

Steady State Kinetics and Insight into Disease Phenotypes. Mutation of highly POOL-ranked residues with large changes in μ_4 values resulted in the least biochemically active enzymes, OTC C303R, H302R, and D263N. OTC C303R was the least active variant with activity below the experimentally determined limit of detection, which is 52 μg citrulline. Even when the enzyme concentration was increased to greater than 1 μM and the reaction time was extended to 1 h, the reaction did not produce sufficient citrulline to be detected. Steady state kinetics assays showed that OTC H302R and OTC D263N were also extremely catalytically deficient. OTC H302R had a 1.3×10^5-fold decrease in activity compared to WT OTC with respect to ORN and a 5.0×10^3-fold decrease with respect to CP whereas OTC D263N had a 3.1×10^5-fold decrease with respect to ORN and 3.3×10^2-fold decrease in activity with respect to CP (Tables 2, 3). C303, D263, and H302 are residues known to be involved in catalysis.[25,27,31] Even OTC H302L, which only had one residue with a μ_4 change greater than 40%, had a 1200- and 89-fold decrease in activity with respect to ORN and CP, respectively.

OTC S267R, C109R, and D196Y were also severely catalytically impaired. OTC S267R had a 1.8×10^3-fold decrease in efficiency with respect to ORN but only a 3.4-fold decrease with respect to CP. S267 is part of the SMG loop which is involved in ORN binding and catalysis. Changing the amino acid from an uncharged serine to a charged arginine clearly impairs catalysis. OTC C109R was also severely catalytically impaired with a 4.9×10^3-fold decrease with respect to ORN and 2.6×10^4-fold decrease in activity with respect to CP. OTC C109R had the largest decrease in activity with respect to CP, which could be because the mutation is at the trimer interface (Figure 1 and Table S1); CP binding

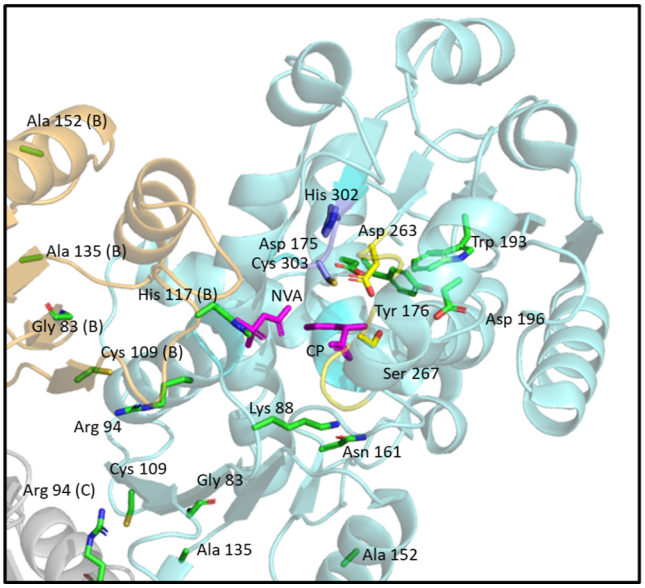

Figure 1. Crystal structure of hOTC (PDB 1c9y)[25] substrates are indicated in pink. The SMG loop is highlighted in yellow. The residues that were mutated based on the μ_4 analysis are highlighted in green, except for the ones that are known to be catalytic residues. D263 and S267 are shown in yellow since they are part of the SMG loop. H302 and C303 are also shown in purple since they important to ornithine binding.

involves H117 from another subunit and therefore a mutation that destabilizes the interface could interfere with CP binding. OTC C109A had essentially unchanged activity relative to WT OTC which suggests that the positive charge from arginine has detrimental effects in that position. OTC D196Y had a 5.7×10^3-fold decrease in activity with respect to ORN and 28-fold decrease in activity with respect to CP. D196 likely helps tether the SMG loop in the correct orientation for catalysis to occur, as it forms a salt bridge with R277, which is located on a short helix adjacent to the SMG loop (Figure 1, yellow).

OTC H117R also was catalytically hindered but to a much less extent, which could be because the mutation maintains the positive charge at this position. The H117R mutation was observed to confer 18% hepatic OTC activity[32] and about 10% activity when expressed and assayed in COS-7 cells.[33] OTC K88N had a 57-fold decrease with respect to ORN and 5.2-fold with respect to CP. It has been shown to confer ~15% activity in cell culture studies.[33] It was previously shown that a positive charge is needed at position 88 for proficient catalytic activity.[34] When the K88Q mutation was made the protein had less than 1% WT activity while K88R mutation retained 20% activity and had no effect on substrate binding.[34] It is believed that acetylation of K88 may inhibit OTC and be a method of physiological regulation.[34] Furthermore, K88 forms a salt bridge with D165, an interaction that may be important for conformational stability. The K88 side chain may help to

https://doi.org/10.1021/acschembio.5c00043
ACS Chem. Biol. 2025, 20, 1059−1067

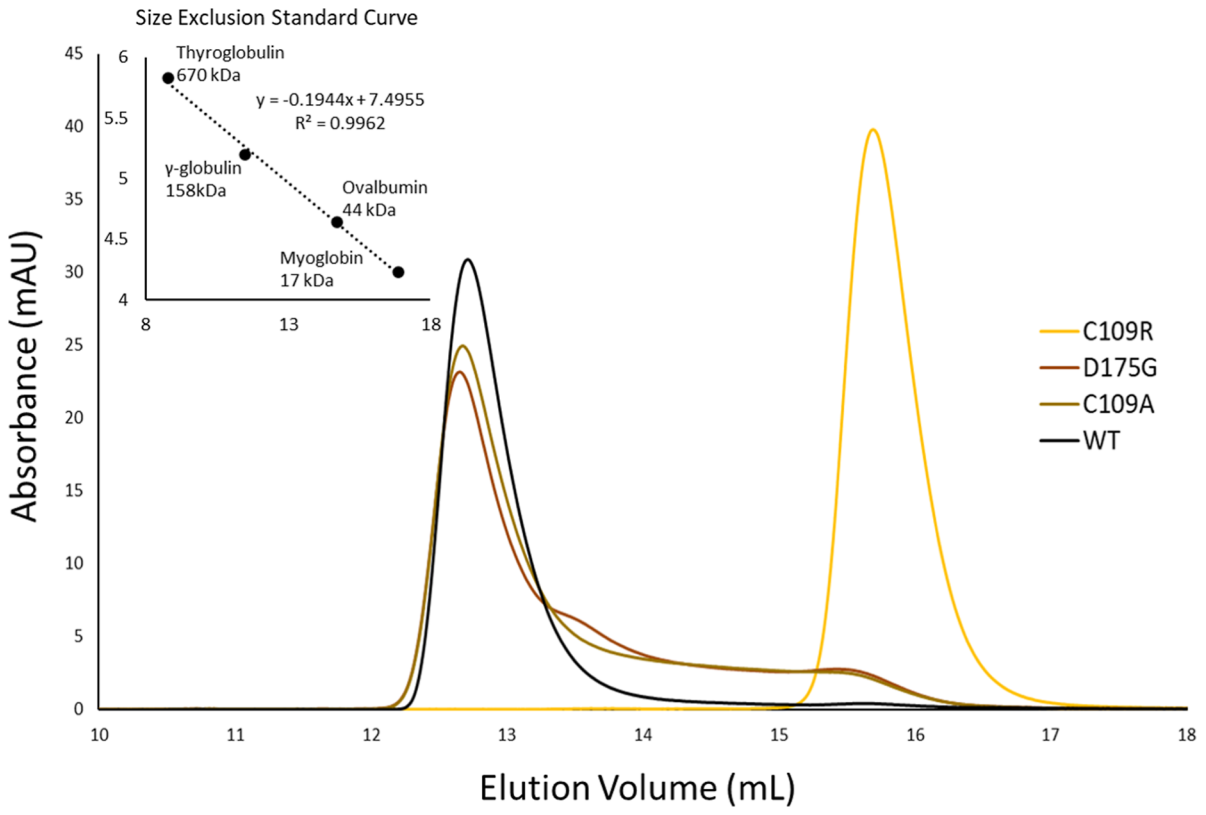

Figure 2. Size exclusion chromatogram comparing WT hOTC, and OTC C109R, C109A, and D175G variants, which were the variants that had the most altered elution profiles.

provide the correct electrostatic environment for the carboxylate moiety of ORN and thus help to orient the bound ORN.

OTC variants G83D, R94T, A135E, A152V, D175G, and Y176C had similar efficiencies as WT OTC. Even though D175 and Y176 were highly POOL ranked, OTC D175G and Y176C variants had overall similar activity to WT OTC; these examples illustrate that small changes in μ_4 values can be good predictors of normal catalytic activity. OTC N161D had the largest single change in μ_4 observed, and a 35-fold decrease in efficiency with respect to ORN and 4.4-fold decrease with respect to CP, which indicates that a very large shift in μ_4 for one important amino acid could predict reduced catalytic activity. Comparison of these results with those from other cell-based assays[7,33] reveals general agreement but with some differences (Table S4). However, μ_4 analysis remains the best predictor of changes in kinetic efficiency.

Thermal Shift Assays of Protein Stability. To understand the effects of these mutations on protein stability, differential scanning fluorimetry was used to determine the melting temperatures of WT OTC and variants in the presence and absence of substrates. Several conditions were tested: Apo, +CP, +ORN, +citrulline (CIT), +phosphate, +norvaline (NVA), +NVA-CP. NVA when combined with CP is considered to be a transition state mimic.[35]

WT Apo OTC had a melting temperature of 59 ± 0.6 °C and most of the disease associated variants had Apo melting temperatures within 4 °C of WT OTC (Figure S2). The variants that had the lowest thermal stability were OTC C109A, C109R, and D175G, which had Apo melting temperatures of 52−54 °C (Figure S5). In the presence of ORN, CIT, or NVA, all the variants showed a similar trend as that of WT OTC, with melting temperatures within a degree of their respective Apo temperatures. This was an expected result since a conformational change initiated by the addition of CP must occur for OTC to bind ORN or NVA. Of note, OTC Y176C exhibited two melting transitions in the presence of NVA, one at 57 ± 0.4 °C and the other at 61 ± 0.1 °C, which suggests that OTC Y176C is able to bind NVA in the absence of CP (Figure S3).

All the variants exhibited the largest change when CP and NVA-CP were added. WT OTC had an increase in melting temperature of 14 °C in the presence of CP. OTC R94T, C109R, H117R, and D196Y had the smallest increases in melting temperature with the addition of CP of 9, 4, 10, and 11 °C, respectively. Additionally, OTC R94T displayed a less steep slope in the melt curve and an altered derivative curve in the presence of CP that was not observed with other variants (Figure S4). The other variants had an increase in melting temperature between 12 and 18 °C with the addition of CP.

In the presence of NVA-CP, WT OTC had an increase in melting temperature of 16 °C compared to Apo temperature and 2 °C compared to CP alone. About half of the variants showed small increases of 1−3 °C in melting temperature in the presence of NVA + CP relative to that with CP alone, with most of the rest showing essentially no change. OTC R94T had a 5 °C increase in melting temperature between +CP and +NVA-CP, which was the largest of the variants. Variants OTC K88N, D196Y, D263N, S267R, H302L, H302R, and C303R did not change melting temperatures with the addition of +NVA-CP relative to their T_m with CP alone (Figure S2). Unfortunately, the yields of N161D and W193R were not sufficient to perform this analysis.

https://doi.org/10.1021/acschembio.5c00043
ACS Chem. Biol. 2025, 20, 1059−1067

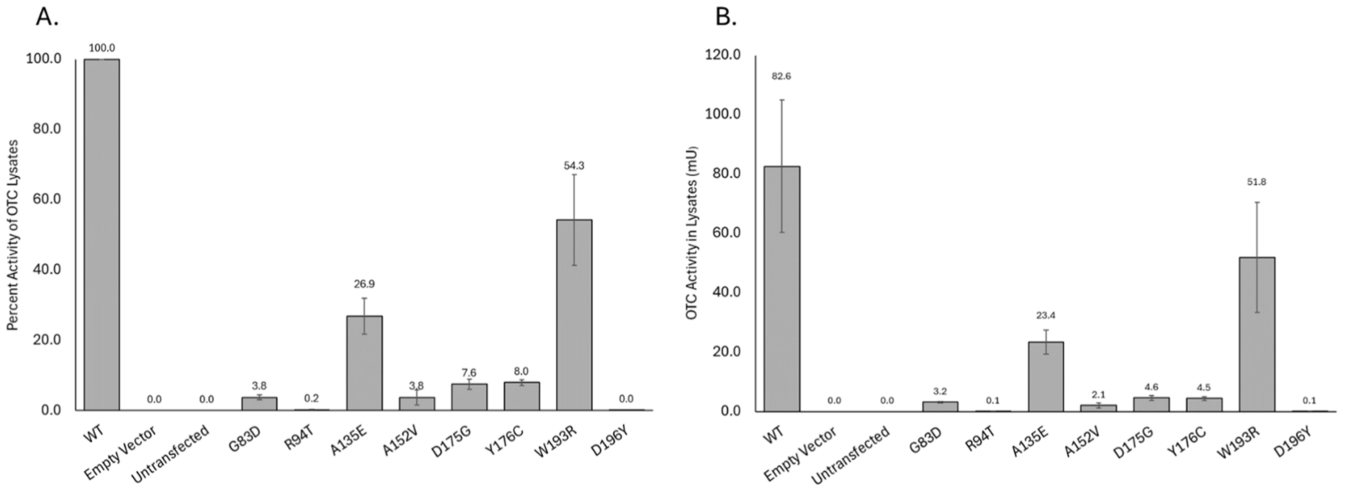

Figure 3. OTC activity is expressed as nmol/min per mg protein which was determined in extracts of cells transfected with various vectors. A. Activity is normalized to percent activity defining WT as 100% activity B. Activity normalized by transfection efficiency.

The addition of phosphate generally increased the melting temperature of these variants between 2 and 5 °C. OTC R94T, C109R (Figure S5), and H302L showed the smallest change in melting temperature with the addition of phosphate, with no or a 1 °C increase from their Apo temperatures.

Size Exclusion Chromatography (SEC) Analysis of OTC. In addition to their stability, the quaternary structures of these OTC variants were also analyzed. We showed previously that SEC can differentiate the monomer vs trimer OTC.[31] Most variants eluted at similar times to WT OTC (Figure S5). The molecular weights of WT OTC and the variants were calculated to be ∼107 kDa, indicating that most of the protein is an intact trimer. OTC C109R was the only variant that eluted as a monomer, at 15.69 mL, which is calculated to be approximately 28 kDa. While this is slightly smaller than the molecular weight of the monomer, it does correlate with the hydrodynamic radius, which is calculated to be 27.3 Å.[31] OTC C109A was used to test whether this was a specific effect of introducing the bulky Arg. Variants OTC C109A and OTC D175G had the most elongated elution profiles (Figure 2). The long trailing tail indicates that although the majority of the protein is present as a trimer, dimer and monomer are both present in the solution. OTC K88N, A152V, and Y176C also have elution profiles consistent with a mixture of trimer, dimer and monomer (Figure S6).

Cell Culture Assays of OTC Activity. To further investigate the functions of these variants, we expressed a subset of them, representing a range of biochemical activities, in human HEK293T cells. OTC variants G83D, R94T, A135E, A152V, D175G, and Y176C all have biochemical activity similar to WT OTC (Tables 2 and 3) and were further studied in cell culture. Untransfected cells and cells with empty vector were used as controls and citrulline formation was not detected with these constructs (Figure 3). OTC D196Y, representing neonatal phenotype, showed large changes in catalytic activity in vitro and was used as the most catalytically compromised variant. Indeed, it had almost no citrulline production (Figure 3).

Although some variants had similar biochemical activity to WT OTC in vitro, they showed a range of activity in the cell culture assay. Indeed, all the variants showed a decrease in activity relative to WT OTC with OTC W193R being the most active variant with 54% of the WT OTC activity. OTC A135E showed activity at 27% the activity of WT OTC. OTC G83D, A152V, D175G, and Y176C variants all had activities of 8% or less than that of WT OTC. OTC R94T had activity that was barely detectable, as did OTC D196Y, a neonatal phenotype variant. The OTC G83D, R94T, A135E, A152V, and Y176C also showed decreased activity in a yeast complementation assay.[7] Cells from a patient with the OTC R94T mutation were previously reported to show virtually no OTC activity.[36] OTC A152V was tested previously in COS-7 cells and displayed 3.7% WT OTC activity, which is similar to our observations (Figure 3).[37]

It is known that OTC biochemical activity levels do not always correlate with activity determined in mammalian expression systems.[37−39] For the severely catalytically deficient enzymes that display the neonatal phenotype, their mechanism of disease is presumably due to this loss of activity; however, many questions remain regarding the female and late-onset phenotypes. It is possible that OTC G83D, D175G, and Y176C variants are unstable and quickly degraded once inside the mitochondrial matrix, similar to OTC A152V.[37] Of the variants assayed in cell culture, stability of OTC G83D, R94T, A135E, A152V, and Y176C was reduced relative to WT OTC (Table 1). OTC Y176C was found to confer an amorphic phenotype with growth <5% of WT in Δ*arg3* yeast, which might be due to the instability of this variant.[7] OTC D175G was calculated to have a more negative ΔΔ*G* than WT OTC (Table 1). However, SEC showed that OTC D175G had a distribution of monomer, dimer, and trimer (Figure 2) and the lowest Apo melting temperature of all the variants tested (Figure S2). OTC D175G also had reduced protein levels in COS-7 cells.[33] D175 is involved in the hydrogen bonding network in the active site and mutating this amino acid affects the stability of the protein.

OTC is expressed as a nuclear gene and must be transported into the mitochondria.[40] Once in the mitochondria it must be assembled into a trimer. G83, A135 and A152 are near the interface between the monomer subunits (Figure 1). It is possible that the mutations prevent efficient oligomerization, resulting in degradation.

CONCLUSIONS

Our study shows that μ_4 analysis correctly predicted, for 17 of 18 variants, the variants that are catalytically deficient in vitro

https://doi.org/10.1021/acschembio.5c00043
ACS Chem. Biol. 2025, 20, 1059−1067

and is a useful tool for studying protein biochemistry. The μ_4 metric differs from most bioinformatics analysis because μ_4 is a chemical property computed from the three-dimensional structure; μ_4 is complementary to using sequence conservation or evolution-based bioinformatics methods. The informatics-based prediction methods were not as good at predicting which variants would have decreased biochemical activity but were able to predict phenotypes more accurately and correlate with our cell culture data.

Most of the neonatal variants with hindered activity were predicted by μ_4 and the bioinformatics servers. Those variants display a large difference from WT OTC with respect to their electrostatic couplings and have high sequence conservation score at the site of mutation. Indeed, OTC N161D, D196Y, and H302R were also all catalytically hindered in vitro and OTC D196Y showed activity below the limit of detection in cell culture. A similar trend was observed with the female variants. Due to the vast differences in phenotype, predicting the severity of late onset phenotypes is difficult for the different prediction algorithms. Understanding the basis for disease for each variant is an important step in the development of personalized interventions.

MATERIALS AND METHODS

Analysis of μ4 Values in Disease Associated Variants of OTC Using POOL and THEMATICS. The biological unit of hOTC (PDB ID 1C9Y; UniProt #P00480)[25] was preprocessed in YASARA[41] to add missing atoms and carry out energy minimization. The prepared OTC PDB file was then imported into the Schrödinger suite of programs. The residue scanning feature was used to build homology models of the disease-associated variants. The PDB files for the variants were then analyzed with POOL, which provides a ranked list of amino acids in the protein in order of their predicted catalytic importance. In addition, POOL provides a moment file, which describes the shape and spread of the first derivative function of the theoretical titration curve for each ionizable amino acid.

The μ_4 values of the known active site residues were compared to those of WT OTC for over 270 disease-associated variants. Variants with changes greater than 20% in μ_4 values of four or more active site residues were compiled. Variants with small changes in the μ_4 (<20%) of four or more catalytic residues were also compiled. Next, we selected variants with both high and low POOL rankings to be represented in both these categories, to determine how POOL ranking at the site of mutation affects the catalytic activity in combination with the μ_4 values. Finally, a variety of phenotypes to represent neonatal, late, and female onset were included in each group. In addition, one variant with the largest change in μ_4 in any one residue was also chosen. A subset of these variants was characterized biochemically.

Site-Directed Mutagenesis, Protein Expression and Purification, and Enzyme Kinetics. The methods were followed as published.[31] A discontinuous colorimetric assay was used to determine the activity of hOTC which was adapted from Ngu and from Mori.[16,40] Detailed procedures are in the Supporting Information.

Differential Scanning Fluorimetry. Melting temperatures of WT hOTC and variants were determined using previously published methods with slight modifications.[16,42] Enzyme (4 μM) was used and final substrate concentrations were 30 mM ORN, 100 mM CP, 10 mM L-norvaline (NVA), 10 mM sodium phosphate and 10 mM Cit. Detailed procedures are in the Supporting Information.

Determination of Molecular Size by Size Exclusion Chromatography. The molecular weights of WT OTC and variants were determined using SEC chromatography using a 26 mL Superdex 200 Increase (Cytiva) column at 0.250 mL/min. An isocratic elution of 50 mM HEPES, 200 mM NaCl, 2 mM EDTA, 2% glycerol, pH 7.4 was used. Gel filtration standards (Bio-Rad 1511901) were characterized in the same buffer to develop a calibration curve, which was used to determine the molecular weights of the proteins.

Site-Directed Mutagenesis and Vector Preparation of Plasmid for Mammalian Cell Culture. A pcDNA3.1(+) IRES-GFP plasmid expressing human OTC was prepared by GenScript. Variants were prepared with Quickchange site-directed mutagenesis kit (Agilent) using mutagenic DNA primers (Eurofins Operon Biotechnologies) and verified by DNA sequencing (Eton Bioscience, Charlestown, MA). Plasmids were prepared using the miraprep protocol.[43] A UV spectrum of each plasmid was obtained to ensure that the A260/280 was >1.6.[44]

Transient Transfection of OTC Proteins, Cell Lysis, and OTC Activity Assay. Transient transfection of HEK293T cells (ATCC CRL-3216) with full-length hOTC was performed as described in the Supporting Information.

After determining transfection efficiency, cells were harvested from the poly-D-lysine coated plates using Gibco TrypLE Express and neutralized with complete serum. The cells were collected by centrifuging at 125*g* for 10 min. The supernatant was decanted, and the pellet was resuspended in mitochondrial lysis buffer. The lysis was performed as published.[38] Citrulline was measured as previously described with a few modifications,[45] including using determination of total protein. A detailed protocol can be found in the Supporting Information.

ASSOCIATED CONTENT

Supporting Information

The Supporting Information is available free of charge at https://pubs.acs.org/doi/10.1021/acschembio.5c00043.

Additional experimental details and methods, additional functional prediction details, DSF and SEC experimental results (PDF)

AUTHOR INFORMATION

Corresponding Authors

Penny J. Beuning − *Department of Chemistry and Chemical Biology and Department of Bioengineering, Northeastern University, Boston, Massachusetts 02115, United States;* orcid.org/0000-0002-7770-022X; Email: beuning@neu.edu

Mary Jo Ondrechen − *Department of Chemistry and Chemical Biology and Department of Bioengineering, Northeastern University, Boston, Massachusetts 02115, United States;* orcid.org/0000-0003-2456-4313; Email: mjo@neu.edu

Authors

Emily Micheloni − *Department of Chemistry and Chemical Biology, Northeastern University, Boston, Massachusetts 02115, United States*

Samantha S. Watson − *Department of Chemistry and Chemical Biology, Northeastern University, Boston, Massachusetts 02115, United States*

Complete contact information is available at: https://pubs.acs.org/10.1021/acschembio.5c00043

Author Contributions

Emily Micheloni: Conceptualization, Methodology, Software, Writing-Reviewing and Editing; Samantha Watson: Conceptualization, Methodology, Software, Writing; Penny Beuning: Supervision, Conceptualization, Writing-Reviewing and Editing; Mary Jo Ondrechen: Supervision, Conceptualization, Computation, Writing-Reviewing and Editing.

https://doi.org/10.1021/acschembio.5c00043
ACS Chem. Biol. 2025, 20, 1059−1067

Funding

This work was supported by the National Science Foundation under grant # MCB-2147498.

Notes

The authors declare no competing financial interest.

■ ACKNOWLEDGMENTS

We gratefully acknowledge Prof. George O'Doherty (Northeastern) for use of his plate reader, Dr. Dashuang Shi (Children's National Medical Center) for the expression plasmid for hOTC, Patrick Sullivan and Oliva Armendarez (Deravi Lab, Northeastern) for their help and use of their fluorescence microscope.

■ REFERENCES

(1) Caldovic, L.; Abdikarim, I.; Narain, S.; Tuchman, M.; Morizono, H. Genotype-Phenotype Correlations in Ornithine Transcarbamylase Deficiency: A Mutation Update. *J. Genet. Genomics* **2015**, *42* (5), 181−194.

(2) Kolansky, D. M.; Conboy, J. G.; Fenton, W. A.; Rosenberg, L. E. Energy-dependent translocation of the precursor of ornithine transcarbamylase by isolated rat liver mitochondria. *J. Biol. Chem.* **1982**, *257* (14), 8467−8471.

(3) (a) Msall, M.; Batshaw, M. L.; Suss, R.; Brusilow, S. W.; Mellits, E. D. Neurologic outcome in children with inborn errors of urea synthesis. Outcome of urea-cycle enzymopathies. *N. Engl. J. Med.* **1984**, *310* (23), 1500−1505. (b) Tuchman, M.; Plante, R. J. Mutations and polymorphisms in the human ornithine transcarbamylase gene: mutation update addendum. *Hum. Mutat.* **1995**, *5* (4), 293−295. (c) Häberle, J.; Rubio, V. Disorders of the Urea CycleUrea Cycle disorders and Related Enzymes. In *Inborn Metabolic Diseases: Diagnosis and Treatment*; Saudubray, J.-M., Baumgartner, M. R., García-Cazorla, A., Walter, J., Eds.; Springer Berlin Heidelberg, 2022; pp 391−405. (d) Lichter-Konecki, U.; Caldovic, L.; Morizono, H.; Simpson, K. Ornithine Transcarbamylase Deficiency. In *GeneReviews(®)*; Adam, M. P., Ardinger, H. H., Pagon, R. A., Wallace, S. E., Bean, L. J. H., Stephens, K., Amemiya, A., Eds.; University of Washington, 1993.

(4) Maestri, N. E.; Lord, C.; Glynn, M.; Bale, A.; Brusilow, S. W. The phenotype of ostensibly healthy women who are carriers for ornithine transcarbamylase deficiency. *Medicine* **1998**, *77* (6), 389−397.

(5) Choi, J. H.; Lee, B. H.; Kim, J. H.; Kim, G. H.; Kim, Y. M.; Cho, J.; Cheon, C. K.; Ko, J. M.; Lee, J. H.; Yoo, H. W. Clinical outcomes and the mutation spectrum of the OTC gene in patients with ornithine transcarbamylase deficiency. *J. Hum. Genet.* **2015**, *60* (9), 501−507.

(6) Rowe, P. C.; Newman, S. L.; Brusilow, S. W. Natural history of symptomatic partial ornithine transcarbamylase deficiency. *N. Engl. J. Med.* **1986**, *314* (9), 541−547.

(7) Lo, R. S.; Cromie, G. A.; Tang, M.; Teng, K.; Owens, K.; Sirr, A.; Kutz, J. N.; Morizono, H.; Caldovic, L.; Ah Mew, N.; et al. The functional impact of 1,570 individual amino acid substitutions in human OTC. *Am. J. Hum. Genet.* **2023**, *110* (5), 863−879.

(8) Stenson, P. D.; Ball, E. V.; Mort, M.; Phillips, A. D.; Shiel, J. A.; Thomas, N. S.; Abeysinghe, S.; Krawczak, M.; Cooper, D. N. Human Gene Mutation Database (HGMD): 2003 update. *Hum. Mutat.* **2003**, *21* (6), 577−581.

(9) Tuchman, M.; Morizono, H.; Reish, O.; Yuan, X.; Allewell, N. M. The molecular basis of ornithine transcarbamylase deficiency: modelling the human enzyme and the effects of mutations. *J. Med. Genet.* **1995**, *32* (9), 680−688.

(10) (a) Tuchman, M.; Morizono, H.; Rajagopal, B. S.; Plante, R. J.; Allewell, N. M. The biochemical and molecular spectrum of ornithine transcarbamylase deficiency. *J. Inherited Metab. Dis.* **1998**, *21* (S1), 40−58. (b) Tuchman, M.; Jaleel, N.; Morizono, H.; Sheehy, L.; Lynch, M. G. Mutations and polymorphisms in the human ornithine transcarbamylase gene. *Hum. Mutat.* **2002**, *19* (2), 93−107.

(11) Yamaguchi, S.; Brailey, L. L.; Morizono, H.; Bale, A. E.; Tuchman, M. Mutations and polymorphisms in the human ornithine transcarbamylase (OTC) gene. *Hum. Mutat.* **2006**, *27*, 626−632.

(12) Tong, W.; Wei, Y.; Murga, L. F.; Ondrechen, M. J.; Williams, R. J. Partial Order Optimum Likelihood (POOL): Maximum likelihood prediction of protein active site residues using 3D structure and sequence properties. *PLoS Comput. Biol.* **2009**, *5* (1), No. e1000266.

(13) Ondrechen, M. J.; Clifton, J. G.; Ringe, D. THEMATICS: A Simple Computational Predictor of Enzyme Function from Structure. *Proc. Natl. Acad. Sci. U.S.A.* **2001**, *98*, 12473−12478.

(14) Capra, J. A.; Laskowski, R. A.; Thornton, J. M.; Singh, M.; Funkhouser, T. A. Predicting protein ligand binding sites by combining evolutionary sequence conservation and 3D structure. *PLoS Comput. Biol.* **2009**, *5* (12), No. e1000585.

(15) (a) Brodkin, H. R.; Novak, W. R.; Milne, A. C.; D'Aquino, J. A.; Karabacak, N. M.; Goldberg, I. G.; Agar, J. N.; Payne, M. S.; Petsko, G. A.; Ondrechen, M. J.; et al. Evidence of the participation of remote residues in the catalytic activity of Co-type nitrile hydratase from *Pseudomonas putida*. *Biochemistry* **2011**, *50* (22), 4923−4935. (b) Somarowthu, S.; Brodkin, H. R.; D'Aquino, J. A.; Ringe, D.; Ondrechen, M. J.; Beuning, P. J. A Tale of Two Isomerases: Compact versus Extended Active Sites in Ketosteroid Isomerase and Phosphoglucose Isomerase. *Biochemistry* **2011**, *50* (43), 9283−9295. (c) Walsh, J. M.; Parasuram, R.; Rajput, P. R.; Rozners, E.; Ondrechen, M. J.; Beuning, P. J. Effects of non-catalytic, distal amino acid residues on activity of *E. coli* DinB (DNA polymerase IV). *Environ. Mol. Mutagen.* **2012**, *53* (9), 766−776. (d) Brodkin, H. R.; DeLateur, N. A.; Somarowthu, S.; Mills, C. L.; Novak, W. R.; Beuning, P. J.; Ringe, D.; Ondrechen, M. J. Prediction of Distal Residue Participation in Enzyme Catalysis. *Protein Sci.* **2015**, *24*, 762−778.

(16) Ngu, L.; Winters, J. N.; Nguyen, K.; Ramos, K. E.; Delateur, N. A.; Makowski, L.; Whitford, P. C.; Ondrechen, M. J.; Beuning, P. J. Probing Remote Residues Important for Catalysis in *Escherichia coli* Ornithine Transcarbamoylase. *PLoS One* **2020**, *15* (2), No. e0228487.

(17) Ko, J.; Murga, L. F.; André, P.; Yang, H.; Ondrechen, M. J.; Williams, R. J.; Agunwamba, A.; Budil, D. E. Statistical criteria for the identification of protein active sites using theoretical microscopic titration curves. *Proteins* **2005**, *59* (2), 183−195.

(18) Coulther, T. A.; Ko, J.; Ondrechen, M. J. Amino acid interactions that facilitate enzyme catalysis. *J. Chem. Phys.* **2021**, *154*, 195101.

(19) Pathira Kankanamge, L. S.; Mora, A.; Ondrechen, M. J.; Beuning, P. J. Biochemical Activity of 17 Cancer-Associated Variants of DNA Polymerase Kappa Predicted by Electrostatic Properties. *Chem. Res. Toxicol.* **2023**, *36*, 1789−1803.

(20) Ng, P. C.; Henikoff, S. Predicting deleterious amino acid substitutions. *Genome Res.* **2001**, *11* (5), 863−874.

(21) (a) Adzhubei, I. A.; Schmidt, S.; Peshkin, L.; Ramensky, V. E.; Gerasimova, A.; Bork, P.; Kondrashov, A. S.; Sunyaev, S. R. A method and server for predicting damaging missense mutations. *Nat. Methods* **2010**, *7* (4), 248−249. (b) Ramensky, V.; Bork, P.; Sunyaev, S. Human non-synonymous SNPs: server and survey. *Nucleic Acids Res.* **2002**, *30* (17), 3894−3900.

(22) Shihab, H. A.; Gough, J.; Cooper, D. N.; Stenson, P. D.; Barker, G. L.; Edwards, K. J.; Day, I. N.; Gaunt, T. R. Predicting the functional, molecular, and phenotypic consequences of amino acid substitutions using hidden Markov models. *Hum. Mutat.* **2013**, *34* (1), 57−65.

(23) Choi, Y.; Sims, G. E.; Murphy, S.; Miller, J. R.; Chan, A. P. Predicting the functional effect of amino acid substitutions and indels. *PLoS One* **2012**, *7* (10), No. e46688.

(24) Pejaver, V.; Urresti, J.; Lugo-Martinez, J.; Pagel, K. A.; Lin, G. N.; Nam, H. J.; Mort, M.; Cooper, D. N.; Sebat, J.; Iakoucheva, L. M.; et al. Inferring the molecular and phenotypic impact of amino acid variants with MutPred2. *Nat. Commun.* **2020**, *11* (1), 5918.

(25) Shi, D.; Morizono, H.; Aoyagi, M.; Tuchman, M.; Allewell, N. M. Crystal structure of human ornithine transcarbamylase complexed

with carbamoyl phosphate and L-norvaline at 1.9 A resolution. *Proteins* **2000**, *39* (4), 271−277.
(26) (a) Couchet, M.; Breuillard, C.; Corne, C.; Rendu, J.; Morio, B.; Schlattner, U.; Moinard, C. Ornithine Transcarbamylase - From Structure to Metabolism: An Update. *Front. Physiol.* **2021**, *12*, 748249. (b) Shi, D.; Morizono, H.; Yu, X.; Tong, L.; Allewell, N. M.; Tuchman, M. Human ornithine transcarbamylase: crystallographic insights into substrate recognition and conformational changes. *Biochem. J.* **2001**, *354*, 501−509. (c) Stebbins, J. W.; Xu, W.; Kantrowitz, E. R. Three residues involved in binding and catalysis in the carbamyl phosphate binding site of *Escherichia coli* aspartate transcarbamylase. *Biochemistry* **1989**, *25*, 2592−2600.
(27) Shi, D.; Morizono, H.; Ha, Y.; Aoyagi, M.; Tuchman, M.; Allewell, N. M. 1.85-A resolution crystal structure of human ornithine transcarbamoylase complexed with N-phosphonacetyl-L-ornithine. Catalytic mechanism and correlation with inherited deficiency. *J. Biol. Chem.* **1998**, *273* (51), 34247−34254.
(28) Ke, H. M.; Lipscomb, W. N.; Cho, Y. J.; Honzatko, R. B. Complex of N-phosphonacetyl-L-aspartate with aspartate carbamoyltransferase. X-ray refinement, analysis of conformational changes and catalytic and allosteric mechanisms. *J. Mol. Biol.* **1988**, *204* (3), 725−747.
(29) Schwarz, J. M.; Cooper, D. N.; Schuelke, M.; Seelow, D. MutationTaster2: mutation prediction for the deep-sequencing age. *Nat. Methods* **2014**, *11* (4), 361−362.
(30) Steinhaus, R.; Proft, S.; Schuelke, M.; Cooper, D. N.; Schwarz, J. M.; Seelow, D. MutationTaster2021. *Nucleic Acids Res.* **2021**, *49*, W446−W451.
(31) Watson, S. S.; Micheloni, E.; Ngu, L.; Barnsley, K. K.; Makowski, L.; Beuning, P. J.; Ondrechen, M. J. Revisiting the roles of catalytic residues in human ornithine transcarbamylase. *Biochemistry* **2024**, *63*, 1858−1875.
(32) Matsuda, I.; Tanase, S. The ornithine transcarbamylase (OTC) gene: mutations in 50 Japanese families with OTC deficiency. *Am. J. Med. Genet.* **1997**, *71* (4), 378−383.
(33) Scharre, S.; Posset, R.; Garbade, S. F.; Gleich, F.; Seidl, M. J.; Druck, A. C.; Okun, J. G.; Gropman, A. L.; Nagamani, S. C. S.; Hoffmann, G. F.; et al. Predicting the disease severity in male individuals with ornithine transcarbamylase deficiency. *Ann. Clin. Transl. Neurol.* **2022**, *9* (11), 1715−1726.
(34) Yu, W.; Lin, Y.; Yao, J.; Huang, W.; Lei, Q.; Xiong, Y.; Zhao, S.; Guan, K. L. Lysine 88 acetylation negatively regulates ornithine carbamoyltransferase activity in response to nutrient signals. *J. Biol. Chem.* **2009**, *284* (20), 13669−13675.
(35) (a) Ha, Y.; McCann, M. T.; Tuchman, M.; Allewell, N. M. Substrate-induced conformational change in a trimeric ornithine-transcarbamoylase. *Proc. Natl. Acad. Sci. U.S.A.* **1997**, *94*, 9550−9555. (b) De Gregorio, A.; Risitano, A.; Capo, C.; Crinio, C.; Petruzzelli, R.; Desideri, A. Evidence of carbamoylphosphate induced conformational changes upon binding to human ornithine carbamoyltransferase. *Biochem. Mol. Biol. Int.* **1999**, *47* (6), 965−970.
(36) Tuchman, M.; Holzknecht, R. A.; Gueron, A. B.; Berry, S. A.; Tsai, M. Y. Six new mutations in the ornithine transcarbamylase gene detected by single-strand conformational polymorphism. *Pediatr. Res.* **1992**, *32* (5), 600−604.
(37) Kogo, T.; Satoh, Y.; Kanazawa, M.; Yamamoto, S.; Takayanagi, M.; Ohtake, A.; Mori, M.; Niimi, H. Expression analysis of two mutant human ornithine transcarbamylases in COS-7 cells. *J. Hum. Genet.* **1998**, *43* (1), 54−58.
(38) Augustin, L.; Mavinakere, M.; Morizono, H.; Tuchman, M. Expression of wild-type and mutant human ornithine transcarbamylase genes in Chinese hamster ovary cells and lack of dominant negative effect of R141Q and R40H mutants. *Pediatr. Res.* **2000**, *48* (6), 842−846.
(39) Morizono, H.; Listrom, C. D.; Rajagopal, B. S.; Aoyagi, M.; McCann, M. T.; Allewell, N. M.; Tuchman, M. 'Late onset' ornithine transcarbamylase deficiency: function of three purified recombinant mutant enzymes. *Hum. Mol. Genet.* **1997**, *6* (6), 963−968.
(40) Mori, M.; Miura, S.; Morita, T.; Takiguchi, M.; Tatibana, M. Ornithine transcarbamylase in liver mitochondria. *Mol. Cell. Biochem.* **1982**, *49* (2), 97−111.
(41) Krieger, E.; Vriend, G. YASARA View - molecular graphics for all devices - from smartphones to workstations. *Bioinformatics* **2014**, *30*, 2981−2982.
(42) Ericsson, U. B.; Hallberg, B. M.; Detitta, G. T.; Dekker, N.; Nordlund, P. Thermofluor-based high-throughput stability optimization of proteins for structural studies. *Anal. Biochem.* **2006**, *357* (2), 289−298.
(43) Pronobis, M. I.; Deuitch, N.; Peifer, M. The Miraprep: A Protocol that Uses a Miniprep Kit and Provides Maxiprep Yields. *PLoS One* **2016**, *11* (8), No. e0160509.
(44) Stuchbury, G.; Munch, G. Optimizing the generation of stable neuronal cell lines via pre-transfection restriction enzyme digestion of plasmid DNA. *Cytotechnology* **2010**, *62* (3), 189−194.
(45) (a) Ceriotti, G. Optimal conditions for ornithine carbamyl transferase determination. A simple micromethod without deproteinization. *Clin. Chim. Acta* **1973**, *47* (1), 97−105. (b) Pierson, M. L.; Cheeke, P. R.; Dickinson, E. O. Resistance of the rabbit to dietary pyrrolizidine (Senecio) alkaloid. *Res. Commun. Chem. Pathol. Pharmacol.* **1977**, *16* (3), 561−564. (c) Suriano, G.; Azevedo, L.; Novais, M.; Boscolo, B.; Seruca, R.; Amorim, A.; Ghibaudi, E. M. In vitro demonstration of intra-locus compensation using the ornithine transcarbamylase protein as model. *Hum. Mol. Genet.* **2007**, *16* (18), 2209−2214.

https://doi.org/10.1021/acschembio.5c00043
ACS Chem. Biol. 2025, 20, 1059−1067